

Low-Cost Direct Torque Control Algorithm for Induction Motor Without AC Phase Current Sensors

Brahim Metidji, *Student Member, IEEE*, Nabil Taib, Lotfi Baghli, *Member, IEEE*, Toufik Rekioua, and Seddik Bacha, *Member, IEEE*

Abstract—This paper presents a novel low-cost and simple phase-current reconstruction algorithm for three-phase induction motor (IM) under direct torque control (DTC) using the information obtained from only one shunt resistor (in series with low-side switches in a conventional three-phase inverter). The aim is to develop a low-cost high-performance IM drive. The proposed algorithm is robust and very simple. It uses the dc current to reconstruct the stator currents needed to estimate the motor flux and the electromagnetic torque. A theoretical concept is developed, the modified look-up table is presented, and current-access tables are designed and used in the phase-current reconstruction. The limitations are also studied and presented.

Simulation and experimental results are given to prove the ability of the proposed scheme of reproducing the performances of a traditional DTC IM drive.

Index Terms—Direct torque control (DTC), induction motor (IM), sensor count reduction, single current sensor.

I. INTRODUCTION

DIRECT torque control (DTC) of induction motors has gained popularity in industrial applications mainly due to its simple control structure from its first introduction in 1986 [1]. An electric motor drive controlled with the DTC technique exhibits performance similar to a field-oriented drive despite a simpler structure [1], [2]. In fact, a DTC scheme achieves the closed-loop control of the motor stator flux and the electromagnetic torque without using any current loop or shaft sensor. Many researchers are interested in this control technique because of its wide area applications used with various ac machine types as induction motor [3], PMSM [4], [5], PM Brushless [6], and reluctance motor [7].

The DTC scheme requires information about the stator currents and the dc-link voltage, which is used with the inverter switches states, to estimate the values of stator flux and elec-

tromagnetic torque. The current feedback for the closed-loop control is usually obtained by sensing instantaneous phase currents by current sensors. In general, galvanically isolated current sensors such as Hall-effect sensors and current transducers are widely used in many applications [8], [9]. They are typically used on, at least, two outputs of the power inverter to provide current feedback signals. Such a kind of sensors performs well, but brings disadvantages to the overall drive system in terms of cost, encumbrance and somehow nonlinearity. Recently, single-current sensor operation has been proposed to reconstruct phase currents from the dc-link current sensor [10]. In this way, various approaches have been proposed in the literature. Some methods adjust the pulse-width modulation (PWM) signals to ensure that two-phase currents can be sampled in each control period [11]–[15]. Other strategies introduce modifications of the modulation algorithm in order to guarantee the reliability of the measurements from the dc-link current sensors under all the operating conditions [16]–[18]. Other interesting approaches are based on the estimation of the motor phase currents using prediction-correction algorithms, thus introducing additional computational burden to the drive system [19]–[22].

Only a few papers deal with the DTC technique for induction motor [23] and PMSM [24]. The algorithm used in these works operates in two stages. First, it predicts the stator currents from a model of the motor and then adjusts the prediction on the basis of the sensed dc-link current. This algorithm requires an additional computation burden and the knowledge of the stator transient inductance.

In this paper, we propose a low-cost single shunt current sensor induction motor (IM) DTC. The stator flux vector and the electromagnetic torque are directly calculated from the voltage and the current derived from a single dc-link voltage sensor (simple voltage divider) and a single dc-link current sensor (simple shunt resistor). The phase currents are estimated by two dc-link current measurement processes. This algorithm does not require additional computation burden or other motor parameter knowledge

II. BASIC DTC OPERATION

DTC uses a simple switching table to determine the most opportune inverter state to attain a desired output torque [1]. By means of current and voltage measurements, it is possible to compute approximately the instantaneous stator flux and output motor torque. The control algorithm based on flux and torque hysteresis controllers determines the voltage required to drive the flux and torque to the desired values within a fixed time period. The fundamental functional blocks used to implement the DTC scheme are represented in Fig. 1.

Manuscript received November 26, 2011; revised January 27, 2012; accepted February 20, 2012. Date of current version May 15, 2012. Recommended for publication by Associate Editor J. O. Ojo.

B. Metidji, N. Taib, and T. Rekioua are with the Laboratoire de Technologie Industrielle et de l'Information, Department of Electrical Engineering, Bejaia University, Bejaia 06000, Algeria (e-mail: metidji77@yahoo.fr; taib_nabil@yahoo.fr; to_reki@yahoo.fr).

L. Baghli is with the Groupe de Recherche en électrotechnique et électronique de Nancy, Université Henri Poincaré, Nancy, France, and also with Laboratoire d'Automatique de Tlemcen, Department of Electrical Engineering, Tlemcen University, Tlemcen 13000, Algeria (e-mail: otfi.baghli@green.uhp-nancy.fr).

S. Bacha is with the G2ELAB, Saint Martin d'Heres 38420, France, and also with University Joseph Fourier, Grenoble 38400, France (e-mail: seddik.bacha@g2elab.inpg.fr).

Color versions of one or more of the figures in this paper are available online at <http://ieeexplore.ieee.org>.

Digital Object Identifier 10.1109/TPEL.2012.2190101

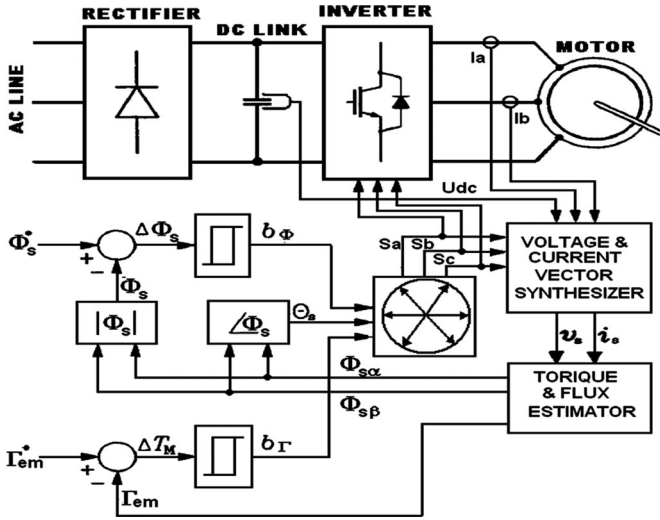


Fig. 1. Basic DTC scheme.

The stator flux vector $\vec{\phi}_s$ and the torque produced by the motor, Γ_{em} , can be estimated using (1) and (2), respectively. These equations only require the knowledge of the previously applied voltage vector V_s , measured stator current I_s , stator resistance R_s , and the motor poles number p .

$$\vec{\phi}_s = \int (\vec{V}_s - R_s \vec{I}_s) dt \quad (1)$$

$$\Gamma_{em} = y_z \text{ with } \vec{y} = \frac{3}{2}p(\vec{\phi}_s \times \vec{I}_s). \quad (2)$$

Once the electromagnetic torque and stator flux magnitude are estimated, a hysteresis control is done and the voltage vectors to be applied are obtained from a switching table.

The stator voltage polar components ($V_{s\alpha}, V_{s\beta}$) on perpendicular (α, β) reference frame result from measured dc-link voltage U_{dc} and the switching controls logical states S_a, S_b , and S_c are given by [1], [2]

$$\begin{cases} V_{s\alpha} = \sqrt{\frac{2}{3}} U_{dc} \left(S_a - \frac{1}{2(S_b + S_c)} \right) \\ V_{s\beta} = \frac{1}{\sqrt{2}} U_{dc} (S_b - S_c) \end{cases} \quad (3)$$

and stator current components ($I_{s\alpha}, I_{s\beta}$)

$$\begin{cases} I_{s\alpha} = \sqrt{\frac{3}{2}} I_a \\ I_{s\beta} = \frac{1}{\sqrt{2}(I_b - I_c)}. \end{cases} \quad (4)$$

The stator resistance can be assumed constant. During a switching period, the voltage vector applied to the motor is constant. By integrating the back electromotive force (EMF), the stator flux can be estimated using (5)

$$\begin{cases} \phi_{s\alpha} = \int (V_{s\alpha} - R_s I_{s\alpha}) dt \\ \phi_{s\beta} = \int (V_{s\beta} - R_s I_{s\beta}) dt. \end{cases} \quad (5)$$

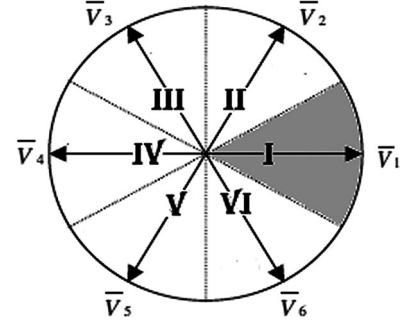


Fig. 2. DTC sectors and inverter voltage vectors.

 TABLE I
 BASIC DTC SWITCHING TABLE

b_Φ	b_Γ	Sect I	Sect II	Sect I	Sect IV	Sect V	Sect VI
1	1	V ₅	V ₆	V ₁	V ₂	V ₃	V ₄
	0	V ₃	V ₄	V ₅	V ₆	V ₁	V ₂
0	1	V ₆	V ₁	V ₂	V ₃	V ₄	V ₅
	0	V ₂	V ₃	V ₄	V ₅	V ₆	V ₁

During the switching period, each voltage vector is constant and (5) is then rewritten as

$$\begin{cases} \phi_{s\alpha} = \phi_{s\alpha} + (V_{s\alpha} - R_s I_{s\alpha}) T_s \\ \phi_{s\beta} = \phi_{s\beta} + (V_{s\beta} - R_s I_{s\beta}) T_s \end{cases} \quad (6)$$

where T_s is the control loop period.

The magnitude of the stator flux can be estimated by

$$\phi_s = \sqrt{\phi_{s\alpha}^2 + \phi_{s\beta}^2}. \quad (7)$$

We can find the flux vector zone using the stator flux components ($\phi_{s\alpha}, \phi_{s\beta}$). By using the flux components, current components and IM number of poles, the electromagnetic torque can be calculated by

$$\Gamma_{em} = \frac{3}{2}p(\phi_{s\alpha} I_{s\beta} - \phi_{s\beta} I_{s\alpha}). \quad (8)$$

As shown in Fig. 2, six equally spaced voltage vectors having the same amplitude and two zero-voltage vectors are the only switching combinations, which can be chosen for an inverter operation. The selection of a voltage vector is made to preserve the torque and the stator flux inside the hysteresis bands limits. The switching table is given by Table I [2].

III. SINGLE CURRENT SENSOR DTC SCHEME

The basic DTC scheme (see Fig. 1) requires two current sensors at least. The proposed DTC scheme described in this paper uses only one shunt resistor for dc-link current measurement as revealed on Fig. 3. For this purpose, a suitable method to reconstruct the phase currents and voltages is devised with a simple modification of the basic DTC scheme using zone shift strategy.

Two modifications of the basic DTC are used for estimating the three-phase currents from a single dc-link current sensor. On the first modification, the control system should be able to generate more voltage vectors. This goal can be achieved

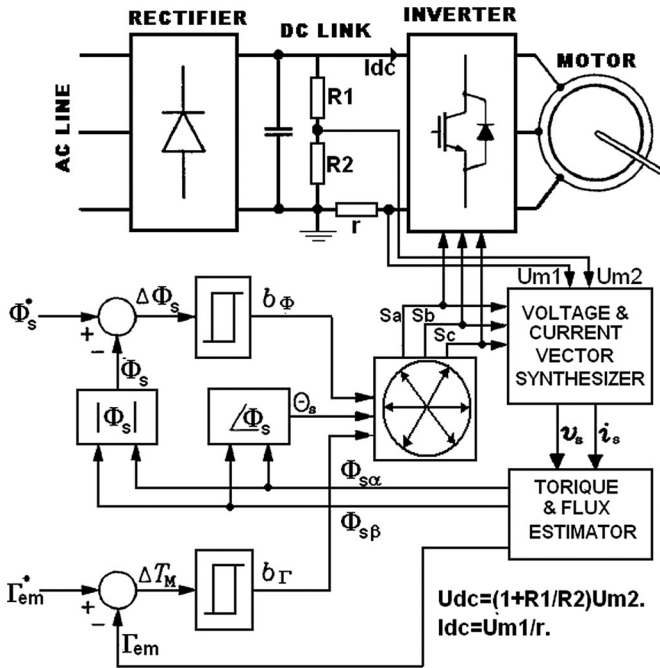


Fig. 3. Proposed DTC scheme.

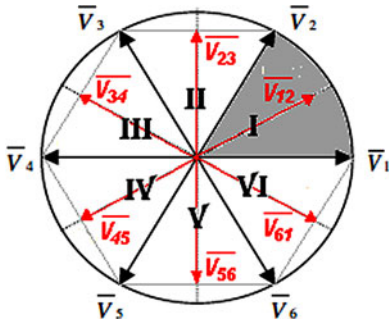


Fig. 4. Proposed DTC sectors and inverter voltage vectors.

approximately by applying, at each cycle period, different voltage vectors for prefixed time intervals, leading to a discrete space vector modulation (DSVM) technique [25], [26]. By using this modulation strategy, new voltage vectors can be synthesized with respect to those used in the basic DTC technique. It has been verified that subdividing the cycle period in two equal time intervals leads to a substantial reduction of current sensors without the need for too complex switching tables. Using the DSVM technique with two equal time intervals, 12 new voltage vectors can be generated; we use only six active voltage vectors in our proposed DTC scheme as represented in Fig. 4. The red vectors represent the synthesized voltage vectors.

As the zone shift strategy, one other modification results in improving the DTC by using a new lookup table and adjusting the six stator flux sectors of the conventional DTC (see Fig. 2). The first sector is taken from 0° to 60° (see Fig. 4), instead of -30° to 30° . The new operation table of the modified DTC is presented in Table II.

TABLE II
PROPOSED DTC SWITCHING TABLE

b_Φ	b_r	Sect I	Sect II	Sect III	Sect IV	Sect V	Sect VI
1	1	V_{56}	V_{61}	V_{12}	V_{23}	V_{34}	V_{45}
	0	V_{34}	V_{45}	V_{56}	V_{61}	V_{12}	V_{23}
0	1	V_{61}	V_{12}	V_{23}	V_{34}	V_{45}	V_{56}
	0	V_{23}	V_{34}	V_{45}	V_{56}	V_{61}	V_{12}

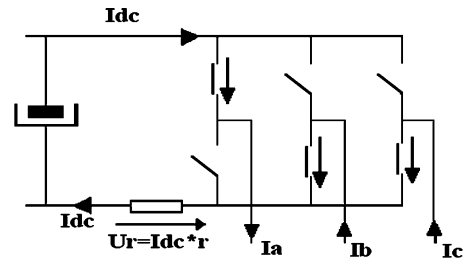


Fig. 5. Inverter currents.

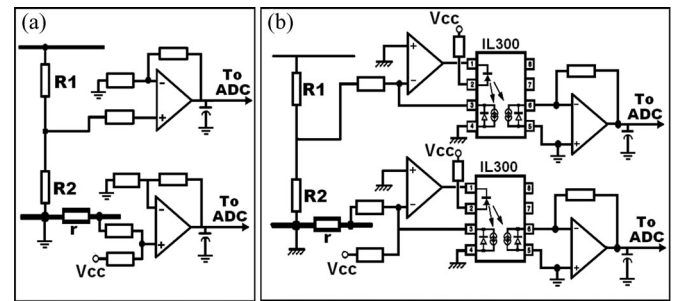


Fig. 6. DC current and dc voltage measurement amplifier. (a) Nonisolated amplifier. (b) Linear photo-isolated amplifier.

IV. DC-LINK CURRENT SAMPLING AND STATOR CURRENT RECONSTRUCTION

One of the most important purposes for single-shunt three-phase reconstruction is to reduce the cost. This, in turn, simplifies the sampling circuit to one shunt resistor and some other electronic components. Moreover, the single-shunt algorithm allows the use of power modules that do not provide, for each phase, individual ground connection.

Another single-shunt measurement advantage is that the same circuit is being used to sense all three phases. For all measurements, the gains and offset will be the same, which eliminate the software calibration of each phase measurement structure.

A. DC Current Measurement

The sampling circuit of dc-link current using single shunt resistor in an usual three-phase power voltage source inverter is depicted in Fig. 5. A measurement shunt resistor is placed between the lower side power switches emitter terminals and the negative dc bus rail that is connected to the ground. The voltage drop across the shunt resistor is amplified and level shifted (see Fig. 6). In the case of nonisolated grounds between control circuit and power circuit, the signal is sent directly to the analog-to-digital converter (ADC) inputs of a digital signal

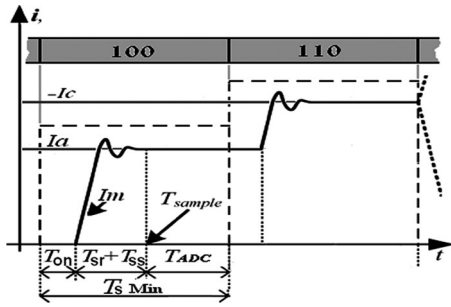


Fig. 7 Recurred sampling time.

controller (DSC), where motor control algorithm is implemented and executed in real time [see Fig. 6(a)]. For more protection, a linear photoisolator amplifier used to isolate the control circuit from power circuit [see Fig. 6(b)].

B. Sampling Time

Both dc-link current sampling instants must be chosen for the application of the three-phase-current reconstruction concept. In accordance with Fig. 7, the optimal sampling instants should be calculated relatively to the active vector transition instants.

For a consistent dc-link current value, the signal sampling must take place after an additional delay

$$T_{\text{sample}} \geq T_{\text{on}} + T_{\text{sr}} + T_{\text{ss}}. \quad (9)$$

The sample time includes the total switching device turn-on delay time T_{on} , the dc-link current signal rise time (T_{sr}), and the signal settling time (T_{ss}). The T_{on} parameter includes the dead-time, the insulated gate bipolar transistor (IGBT) driver signal processing time, and the worst case switching device (IGBT) on-time delay. The parameter T_{ss} is related to the signal amplifiers and the isolation circuit.

Once the sampling is started, the process requires an extra sample-and-hold time delay (T_{ADC}). The latter can be important, particularly in the case of a low-cost DSC ADC. However, all these delays may be neglected compared to the DTC control period. The sampling instant chosen in the proposed phase-current reconstruction is at the end of each half period when the dc current signal is stabilized.

The smallest DTC control period is given by

$$T_s \geq 2(T_{\text{on}} + T_{\text{sr}} + T_{\text{ss}} + T_{\text{ADC}}) \quad (10)$$

Actually, the sum of all these time delays is about a few microseconds, even with the isolation system, which is far smaller compared to $50 \mu\text{s}$ used in our system. Fig. 8 illustrates the example of recurred sampling time when the voltage vector V_{12} is applied.

C. Phase Current Reconstruction

In the classical DTC, for each active voltage vector, there is only one current flowing in the dc link, which could be measured. Table III illustrates according to the switch states the relationship between the dc-link current and the phase currents.

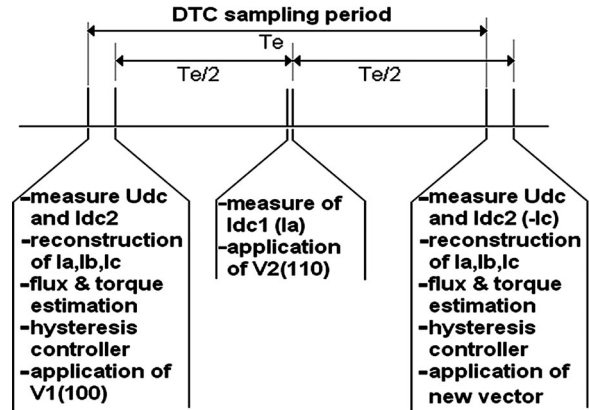
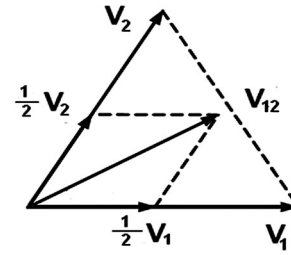

 Fig. 8. Two interval DSVM DTC and phase currents reconstruction example with the application of V_{12} voltage vector.

 TABLE III
PHASE CURRENT MEASURED IN EACH CLASSIC DTC VOLTAGE VECTOR

Active Voltage Vector	DC-link Current
V_1	I_a
V_2	$-I_c$
V_3	I_b
V_4	$-I_a$
V_5	I_c
V_6	$-I_b$

 TABLE IV
PHASE CURRENT MEASURED IN EACH PROPOSED DTC VOLTAGE VECTOR

Active Voltage Vector	1 st interval DC-link Current	2 nd interval DC-link Current
V_{12}	I_a	$-I_c$
V_{23}	$-I_c$	I_b
V_{34}	I_b	$-I_a$
V_{45}	$-I_a$	I_c
V_{56}	I_c	$-I_b$
V_{61}	$-I_b$	I_a

By using the two-interval discrete space vector modulation, for each one of the new six active vectors, we can reconstruct the three-phase motor currents (see Table IV).

From Table IV, it is clear that by knowing the inverter switch position in two intervals of each period the actual currents for two phases can be obtained without further computing process. Assuming that, $I_{\text{dc}1}$ is the dc-link current measured at the end of the first interval and $I_{\text{dc}2}$ is the one measured at the second half interval, are summarized in Table V, the three-phase motor currents I_a , I_b , and I_c are given in function of voltage vector and the dc-link current. A phase-current reconstruction time

TABLE V
PHASE CURRENT RECONSTRUCTION RELATIONSHIP FOR EACH
VOLTAGE VECTOR

Voltage Vector	Ia	Ib	Ic
V ₁₂	Idc ₁	Idc ₂ -Idc ₁	-Idc ₂
V ₂₃	Idc ₁ -Idc ₂	Idc ₂	-Idc ₁
V ₃₄	-Idc ₂	Idc ₁	Idc ₂ -Idc ₁
V ₄₅	-Idc ₁	Idc ₁ -Idc ₂	Idc ₂
V ₅₆	Idc ₂ -Idc ₁	-Idc ₂	Idc ₁
V ₆₁	Idc ₂	-Idc ₁	Idc ₁ -Idc ₂

sequence example with the application of V₁₂ voltage vector is presented in Fig. 8.

D. Motor Speed Range

In two-interval DSVM, one sampling period is divided into two equal time intervals (see Fig. 8). One of the VSI voltage vectors is applied to each of them. The number of voltage vectors that can be generated is 14 vectors. The proposed low-cost DTC algorithm uses only six voltage vectors out of them which can be used for phase-current reconstruction.

The magnitude of the generated voltage vector V₁ using the classical DTC algorithm can be written as

$$|V_1| = \frac{2}{3}U_{dc}. \quad (11)$$

The generated voltage vector V₁₂ using the proposed DSVM DTC algorithm is given by

$$|V_{12}| = \frac{2}{3}U_{dc} \cos \frac{\pi}{6} = \frac{1}{\sqrt{3}}U_{dc}. \quad (12)$$

The vector voltage magnitude ratio is given by

$$r = \frac{|V_{12}|}{|V_1|} = \frac{\sqrt{3}}{2}. \quad (13)$$

Speed control is achieved by means of variable frequency. Apart from frequency, the applied voltage needs to be varied because the stator flux magnitude is kept constant by the DTC control.

Neglecting the stator resistance drop, we can consider that the voltage magnitude, in steady state, is given by

$$V_{sn} \approx \varphi_{sn}\omega_s \quad (14)$$

Reducing the voltage maximum magnitude will reduce the rotational components of the back EMF, leading to a reduction in the maximum stator pulsation and hence to the speed range. The maximum motor speed with the proposed algorithm is limited to 86% compared to the original DTC control algorithm.

V. SIMULATION RESULTS

MATLAB/SIMULINK model-based on power system toolbox was developed to examine the proposed control algorithm and the phase-current reconstruction feasibility.

The parameters of the induction motor used in this study are as follows:

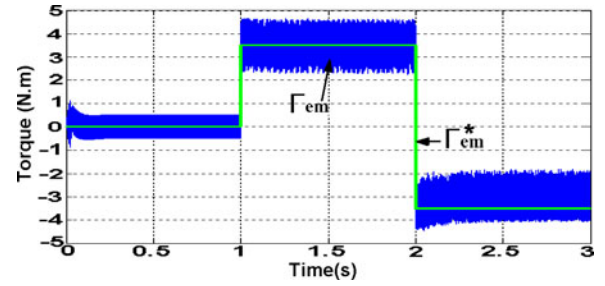


Fig. 9. Torque dynamic.

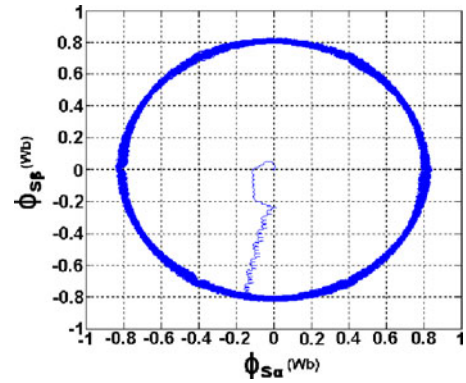


Fig. 10. Stator flux circular trajectory.

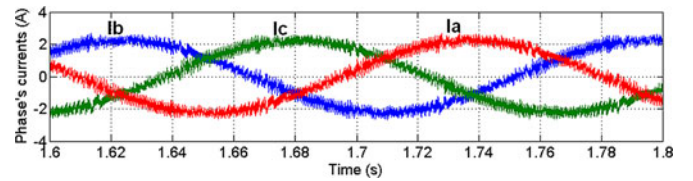


Fig. 11. Measured phase currents.

$P_n = 1.1 \text{ kW}$, $U_n = 415 \text{ V}$, $f = 50 \text{ Hz}$, $\Omega_n = 1415 \text{ r/min}$, $R_s = 6.03 \Omega$, $R_r = 6.085 \Omega$, $L_{ls} = 29.9 \text{ mH}$, $L_{lr} = 29.9 \text{ mH}$, $L_m = 489.3 \text{ mH}$, $J = 0.011787 \text{ Kg.m}^2$.

The adopted sampling interval value of the DTC algorithm in the simulations is $100 \mu\text{s}$ (10 kHz).

Fig. 9 shows the variations of the motor torque in the proposed control scheme. First, the machine is fluxed with a zero-reference torque, then at 1s, we set the torque reference to 3.5 Nm (50% of the rated torque) and a torque inversion is made at 2s. The flux reference value is set to 0.8 Wb. One can see that the torque presents good dynamics. The $\phi_{s\alpha}$ and $\phi_{s\beta}$ circular trajectory is presented in Fig. 10.

Figs. 11 and 12 illustrate the measured and the reconstructed phase currents, respectively. One can see that the three waveforms are similar.

Fig. 13 presents the simulation results of the phase current dynamics during torque reversal. We can see that the change in the three currents I_a , I_b , and I_c caused by the torque reversal is very fast.

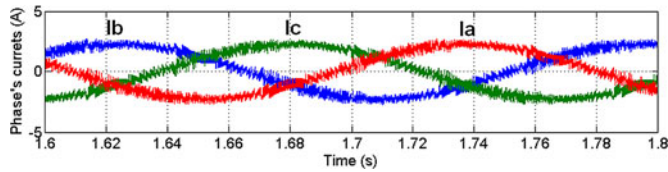


Fig. 12. Reconstructed phase currents.

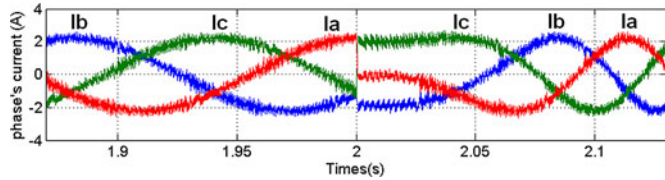


Fig. 13. Phase currents dynamic during torque reversal.

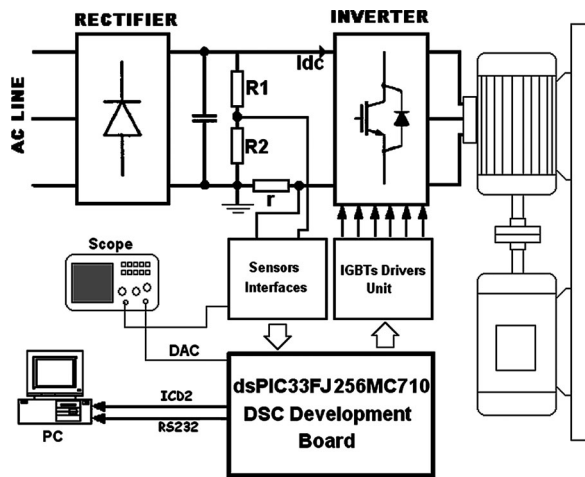


Fig. 14. Experimental setup.

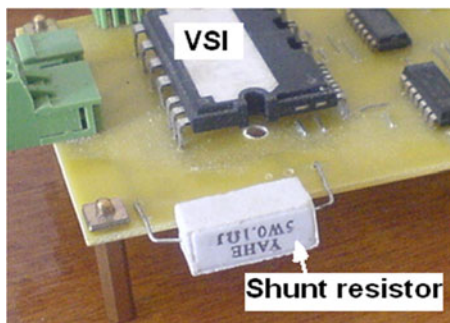


Fig. 15. Power converter and the shunt resistance.

VI. EXPERIMENTAL RESULTS

To verify the computer simulation results, the proposed control method was applied in a DTC experimental test setup. The experimental setup, which is depicted in Figs. 14 and 15, consists of a 1.1-kW induction motor, an IGBT VFI and a dsPIC 33FJ256MC710 DSC-based controller. The induction motor has the same parameters as those of the simulation model. The dc bus voltage and current were interfaced into the controller through an analog to digital (A/D) converter built into the DSC board.

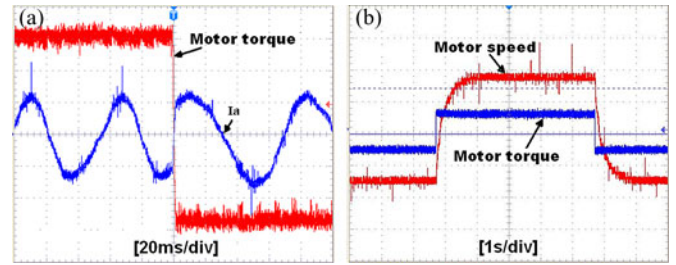


Fig. 16. (a) Motor torque and stator current (1 N·m/div, 1 A/div). (b) Motor torque and speed (5 N·m/div, 100 r/min/div).

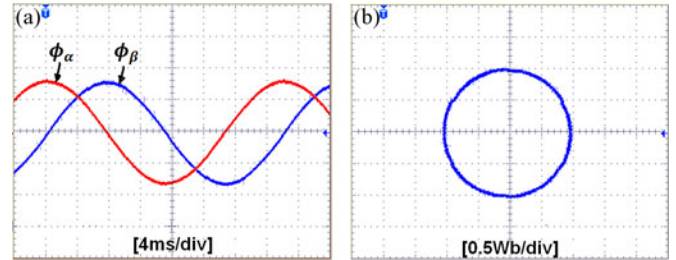


Fig. 17. (a) Stator flux components and (b) its circular trajectory.

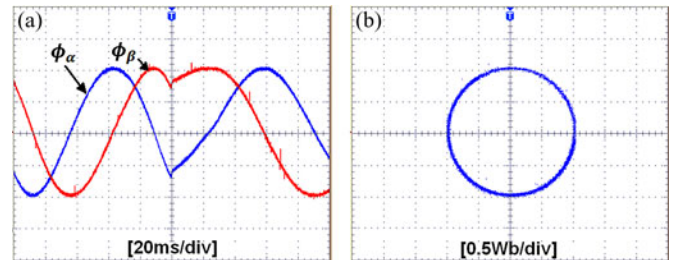


Fig. 18. (a) Stator flux components and (b) its circular trajectory during torque reversal.

The sampling frequency is set to 9 kHz and the DSC board was controlled thanks to a PC.

Fig. 16(a) shows the torque waveform, and the phase “a” stator motor current for the torque reference step between 3 Nm to -3 Nm. Fig. 16(b) presents the motor speed transient response when the torque reference step is applied. One can see that the control of the torque is achieved as expected, and when the torque is inverted, the motor changes the rotation direction.

The stator flux components and its locus during a normal and torque reversal operations are presented in Figs. 17 and 18, respectively. It can be seen that the control of the flux is achieved as expected, and in the torque reversal instance the stator flux vector changes its direction i.e., $\phi_{s\alpha}$ is lagging the $\phi_{s\beta}$.

Fig. 19 illustrates the experimental results of the stator flux sector and its corresponding voltage vector. The selected voltage vector depends on the stator flux sector and the flux and torque hysteresis controller output [see Fig. 19(a)], whereas Fig. 19(b) shows the stator flux sector and its corresponding voltage vector without torque control.

Fig. 20 shows the measured and the reconstructed motor current waveforms for the modified control method. The zoomed measure and reconstructed phase “a” motor current presented

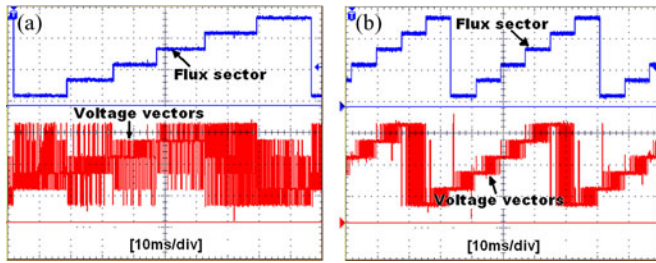


Fig. 19. Flux sector (flux sector index: 2/div) and its corresponding voltage vector (voltage vector index: 2/div). (a) Torque and flux control. (b) Flux control.

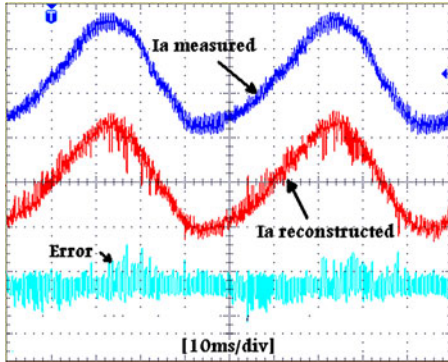


Fig. 20. Measured and reconstructed phase "a" current (2 A/div).

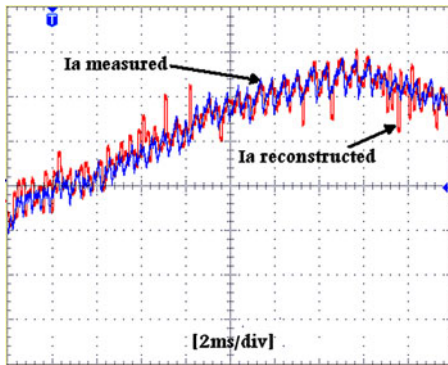


Fig. 21. Zoomed window of measured and reconstructed phase "a" current (1 A/div).

on Fig. 21 confirms the effectiveness of the proposed method to reduce the DTC scheme cost by replacing all galvanic sensors (current and voltage Hall-Effect sensors) with only one shunt resistor and one voltage divider.

Fig. 22(a) illustrates the dc-link current and phase "a" motor current, and its zoom is presented in Fig. 22(b), where we can clearly see the intervals used to sense the phase "a" current directly. In this example, the voltage vector sequence applied to motor are V_{61} , V_{12} , V_{12} , V_{12} , V_{34} , V_{61} , V_{61} , V_{12} , V_{12} , and V_{12} . As a result, the current measured for each period from the dc current can be written as a sequence of current pair $(-I_b, I_a)$, $(I_a, -I_c)$, $(I_a, -I_c)$, $(I_a, -I_c)$, $(I_b, -I_a)$, $(-I_b, I_a)$, $(-I_b, I_a)$, $(I_a, -I_c)$, $(I_a, -I_c)$, and $(I_a, -I_c)$. If the stator flux sector is not changed, then we can determine from Table II that there are only two possible sectors (see Sector II or Sector V).

The Fig. 23(a) shows the stator current dynamic during the torque reversal and its zoom is presented in Fig. 23(b). One can

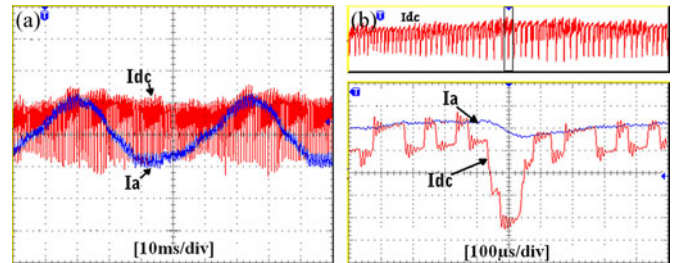


Fig. 22. The measured dc-link current and its zoom and the zoom of phase "a" current (2 A/div).

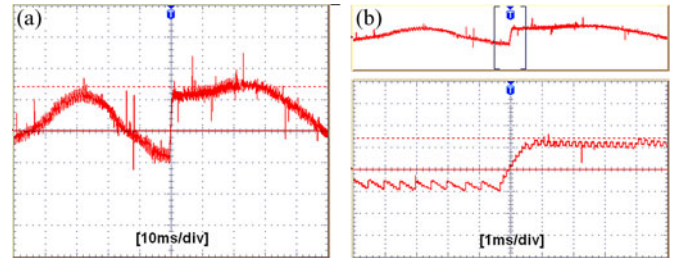


Fig. 23. The stator current dynamic during (a) torque reversal and (b) its zoom (2 A/div).

observe that the stator current transition is not instant, but there is a delay depending on the stator leakage inductance.

VII. CONCLUSION

In this paper, a new low-cost DTC scheme for IM drives has been presented using a single shunt resistor inserted in the dc-link path, for phase-current reconstruction.

The proposed method reconstructs the stator currents needed to estimate the stator flux magnitude and the electromagnetic motor torque, by means of a simple modification in the basic DTC scheme; 30° zone shift strategy is applied. To generate the six active voltage vector needed for dc-link current measure without changing the DTC strategy, a two-intervals discrete space vector modulation technique is used.

The effectiveness of the proposed DTC algorithm using a single shunt resistor was verified by computer simulations and experimentally on a three-phase induction motor, rated at 1.1 kW. The results presented have demonstrated that beyond the small reduction of the motor speed range, the phase currents reconstructed are very close to the measured phase currents, with an excellent performance of the drive system, nearly identical to that achieved with the traditional DTC scheme.

REFERENCES

- [1] I. Takahashi and T. Noguchi, "A new quick-response and high-efficiency control strategy of an induction motor," *IEEE Trans. Ind. Appl.*, vol. IA-22, no. 5, pp. 820–827, Sep./Oct. 1986.
- [2] S. A. Zaid, O. A. Mahgoub, and K. El-Metwally, "Implementation of a new fast direct torque control algorithm for induction motor drives," *IET Electr. Power Appl.*, vol. 4, no. 5, pp. 305–313, May 2010.
- [3] C. Patel, R. P. P. A. Day, A. Dey, R. Ramchand, K. K. Gopakumar, and M. P. Kazmierkowski, "Fast direct torque control of an open-end induction motor drive using 12-sided polygonal voltage space vectors," *IEEE Trans. Power Electron.*, vol. 27, no. 1, pp. 400–410, Jan. 2012.
- [4] Y. Zhang and J. Zhu, "Direct torque control of permanent magnet synchronous motor with reduced torque ripple and commutation frequency," *IEEE Trans. Power Electron.*, vol. 26, no. 1, pp. 235–248, Jan. 2011.

- [5] Y. Zhang and J. Zhu, "A novel duty cycle control strategy to reduce both torque and flux ripples for DTC of permanent magnet synchronous motor drives with switching frequency reduction," *IEEE Trans. Power Electron.*, vol. 26, no. 10, pp. 3055–3067, Oct. 2011.
- [6] K. D. Hoang, Z. Q. Zhu, and M. P. Foster, "Influence and compensation of inverter voltage drop in direct torque-controlled four-switch three-phase PM brushless AC drives," *IEEE Trans. Power Electron.*, vol. 26, no. 8, pp. 2343–2357, Aug. 2011.
- [7] S. Bolognani, L. Peretti, and M. Zigliotto, "Online MTPA control strategy for DTC synchronous-reluctance-motor drives," *IEEE Trans. Power Electron.*, vol. 26, no. 1, pp. 20–28, Jan. 2011.
- [8] G. Foo and M. F. Rahman, "Direct torque and flux control of an IPM synchronous motor drive using a backstepping approach," *IET Elect. Power Appl.*, vol. 3, no. 5, pp. 413–421, Sep. 2009.
- [9] M. E. Haque and M. F. Rahman, "Incorporating control trajectories with the direct torque control scheme of interior permanent magnet synchronous motor drive," *IET Elect. Power Appl.*, vol. 3, no. 2, pp. 93–101, Mar. 2009.
- [10] T. C. Green and B. W. Williams, "Derivation of motor line-current waveforms from the dc-link current of an inverter," in *Proc. IEE Elect. Power Appl.*, Jul. 1989, vol. 136, no. 4, pt. B, pp. 196–204.
- [11] W. C. Lee, T. K. Lee, and D. S. Hyun, "Comparison of single-sensor current control in the dc link for three-phase voltage-source PWM converters," *IEEE Trans. Ind. Electron.*, vol. 48, no. 3, pp. 491–505, Jun. 2001.
- [12] J. T. Boys, "Novel current sensor for PWM AC drives," in *Proc. Electr. Power Appl.*, 1988, vol. 135, pt. B, pp. 27–32.
- [13] F. Petruzzello, G. Joos, and P. D. Ziogas, "Some implementation aspects of line current reconstruction in three phase PWM inverters," in *Proc. 16th IEEE Annu. Conf. Ind. Electron. Soc.*, Pacific Grove, CA, 27–30 Nov. 1990, pp. 1149–1154.
- [14] F. Blaabjerg and J. K. Pedersen, "An ideal PWM-VSI inverter using only one current sensor in the dc-link," in *Proc. 5th Int. Conf. Power Electron. Variable-Speed Drives*, London, U.K, 26–28 Oct. 1994, pp. 458–464.
- [15] F. Blaabjerg, J. K. Pedersen, U. Jaeger, and P. Thøgersen, "Single current sensor technique in the DC link of three-phase PWM-VS inverters: A review and a novel solution," *IEEE Trans. Ind. Appl.*, vol. 33, pp. 1241–1253, 1997.
- [16] H.-G. Joo, M.-J. Youn, and H.-B. Shin, "Estimation of phase currents from a DC-Link current sensor using space vector PWM method," *Electr. Mach. Power Syst.*, vol. 28, pp. 1053–1069, 2000.
- [17] J. F. Moynihan, S. Bolognani, R. C. Kavanagh, M. G. Egan, and J. M. D. Murphy, "Single sensor current control of AC servo drives using digital signal processors," in *Proc. 5th Eur. Conf. Power Electron. Appl.*, Brighton, U.K, Sep. 1993, vol. 4, pp. 415–421.
- [18] M. Riese, "Phase current reconstruction of a three-phase voltage source inverter fed drive using a sensor in the dc link," in *Proc. Power Convers. Intell. Motion Conf.*, 1996, pp. 95–101.
- [19] T. M. Wolbank and P. Macheiner, "An improved observer-based current controller for inverter fed AC machines with single DC-link current measurement," in *Proc. IEEE Power Electron. Spec. Conf.*, Cairns, Australia, 23–27 Jun. 2002, pp. 1003–1008.
- [20] T. M. Wolbank and P. Macheiner, "Scheme to reconstruct phase current information of inverter fed AC drives," *IEE Electron. Lett.*, vol. 38, no. 5, pp. 204–205, 2002.
- [21] T. M. Wolbank and P. Macheiner, "Current controller with single DC link current measurement for inverter fed AC machines based on an improved observer structure," *IEEE Trans. Power Electron.*, vol. 19, no. 6, pp. 1526–1527, 2004.
- [22] H. Kim and T. M. Jahns, "Phase current reconstruction for AC motor drives using a DC link single current sensor and measurement voltage vectors," *IEEE Trans. Power Electron.*, vol. 21, no. 5, pp. 1413–1419, 2006.
- [23] M. Bertoluzzo, G. Buja, and R. Menis, "Direct torque control of an induction motor using a single current sensor," *IEEE Trans. Ind. Electron.*, vol. 53, no. 3, pp. 778–784, Jun. 2006.
- [24] E. Peralta-Sanchez, F. Al-rifai, and N. Schofield, "Direct torque Control of permanent magnet motors using a single current sensor," in *Proc. Electr. Mach. Drives Conf.*, Miami, FL, 3–6 May, 2009, pp. 89–94.
- [25] T. G. Habetler and D. M. Divan, "Control strategies for direct torque control using discrete pulse modulation," *IEEE Trans. Ind. Appl.*, vol. 27, no. 5, pp. 893–901, Sep./Oct. 1991.
- [26] D. Casadei, G. Serra, and A. Tani, "Implementation of a direct torque control algorithm for induction motors based on discrete space vector modulation," *IEEE Trans. Power Electron.*, vol. 15, no. 4, pp. 769–777, Jul. 2000.



Brahim Metidji (M'12) was born in Bouira, Algeria, in 1977. He received the M.S. degree in electrical engineering in 2004 from the A/Mira University of Bejaia, Bejaia, Algeria, where he is currently working toward the Ph.D. degree in electrical engineering at the Department of Electrical Engineering.

His research interests include variable-speed ac motor drives and power converter in particular the matrix converter.



Nabil Taib was born in Béjaia, Algeria, in 1977. He received the M.S. degree in electrical control systems from the University of Bejaia, Bejaia, in 2004, where he is currently working toward the Ph.D. degree in electrical engineering at the Department of Electrical Engineering.

In 2009, he was a Lecturer in the Electrical Engineering Department, A.Mira of Bejaia, Bejaia. His research interests are focused on the applications of the matrix converters in the renewable energy systems.

Mr. Taib is a member of the editorial board of the *International Journal of Computer Science and Emerging Technologies*.



Lotfi Baghli (M'12) was born in 1971. He received the Diploma degree (with Hons.) in electrical engineering from the Ecole Nationale Polytechnique of Algiers, Algiers, Algeria, in 1994, and the DEA degree in electrical engineering from the Université Henri Poincaré, Nancy, France, in 1995 and 1999, respectively.

He was a Lecturer at Nancy Université and a member of Groupe de Recherche en Electrotechnique et Electronique de Nancy. He is currently a Visiting Lecturer at Tlemcen University, Tlemcen, Algeria.

His research interests include digital control using DSP, PSO, and genetic algorithms applied to the control and identification of electrical machines.



Toufik Rekioua received the engineering degree from the National Polytechnic Institute of Algiers, Algiers, Algeria, and the Doctoral degree from the Institut National Polytechnique de Lorraine, Nancy, France, in 1991.

Since 1992, he has been a Professor in the Department of Electrical Engineering, University of Bejaia, Bejaia, Algeriawhere he is currently the Director of the LTII laboratory. His research activities include control of electrical drives, modeling, wind turbine, and control in ac machines.



Seddik Bacha (M'08) received the Engineering and Master's degrees from the National Polytechnic Institute of Algiers, Algiers, Algeria, in 1982 and 1990, respectively, and the Ph.D. and HDR degrees from the Laboratory of Electrical Engineering of Grenoble, G2Elab, Saint Martin d'Heres, France, in 1993 and 1998, respectively.

He is currently the Manager of Power System Group, G2Elab and a Professor at the University Joseph Fourier, Grenoble, France. His main research interests include renewable integration and power

quality.